

Don't bleach chaotic data

James Theiler

Center for Nonlinear Studies and Theoretical Division, Los Alamos National Laboratory, Los Alamos, NM 87545; and Santa Fe Institute, 1660 Old Pecos Trail, Santa Fe, NM 87501.

Stephen Eubank

Center for Nonlinear Studies and Theoretical Division, Los Alamos National Laboratory, Los Alamos, NM 87545; Santa Fe Institute, 1660 Old Pecos Trail, Santa Fe, NM 87501; and Prediction Company, 320 Aztec Street, Santa Fe, NM 87501.

(Received 10 July 1992; accepted for publication 11 August 1993)

A common first step in time series signal analysis involves digitally filtering the data to remove linear correlations. The residual data is spectrally white (it is “bleached”), but in principle retains the nonlinear structure of the original time series. It is well known that simple linear autocorrelation can give rise to spurious results in algorithms for estimating nonlinear invariants, such as fractal dimension and Lyapunov exponents. In theory, bleached data avoids these pitfalls. But in practice, bleaching obscures the underlying deterministic structure of a low-dimensional chaotic process. This appears to be a property of the chaos itself, since nonchaotic data are not similarly affected. The adverse effects of bleaching are demonstrated in a series of numerical experiments on known chaotic data. Some theoretical aspects are also discussed.

I INTRODUCTION

Much of the current interest in nonlinear signal processing arises not so much as an extension of linear analysis, but from the recognition that an entirely new idea — chaos — will play a significant role. In some cases, this entirely new idea has led to entirely new techniques for time series analysis. These have provided experimentalists with new ways to understand the implications of their data, though the limitations of these new technologies have not always been understood or well appreciated. In other cases, chaos has shed new light on the interpretation of conventional time series analysis tools (for instance, by providing a deterministic explanation for broadband spectra). Our intent here is to investigate the limitations of one of these conventional tools in the context of chaotic time series.

Bleaching, or “pre-whitening,” is the process of linearly filtering time series data to remove autocorrelation — that is, to make the power spectrum more nearly flat, or “white.” As a first step in time series analysis, it is a time-honored practice among statisticians [1–4] and statistics-minded economists [5–10]. Even the classic treatise of Blackman and Tukey [11] recommends “preemphasis” of a signal to make the spectrum “more nearly constant.” It is an initially attractive procedure because it eliminates autocorrelation, which is one of the major sources of artifact in nonlinear time series analysis [12–16]. Further, since bleaching is accomplished with a finite order non-recursive (or finite-impulse-response, or FIR) filter, it can be proven that the nonlinear properties (such as dimension and Lyapunov exponent) remain invariant [6, 17–21].

However, this theoretical invariance does not always carry over to practical data analysis. It has long been known that recursive (or infinite-impulse-response, or IIR) filters can — in practice and in principle — change the character of a nonlinear process, as inferred from its time series [22, 23]. Mitschke [24] suggested that

acausal IIR filters might be less destructive, though others [16, 21] have shown that these too can change the nonlinear invariants. Insofar as FIR filters approximate IIR filters, their effects can be similarly detrimental: a graphic demonstration is provided in Ref. [19]. In an earlier paper [25], we briefly noted that bleaching with very high order linear filters can degrade evidence for nonlinearity in a time series. In this paper, that observation is extended. Even when the bleaching is constrained to relatively low order (by the Akaike criterion, for instance), and even for tasks other than detecting nonlinear structure, we find that the effect of bleaching on chaotic data can be detrimental. On the other hand, bleaching *nonchaotic* data does *not* have such a negative effect.

After introducing the bleaching process in Sect. II, the effect of bleaching on chaotic data is demonstrated numerically, first by looking at the problem of nonlinear prediction (in Sect. III), then by comparing residual-based to surrogate data approaches for detecting nonlinearity in time series (in Sect. IV). These numerical results lead us to argue against pre-whitening chaotic data; however, in Sect. V, this view is tempered by showing that some linear prefiltering can still be advantageous. The emphasis in this paper is on numerical results, but in Sect. VI some theoretical issues are discussed: the limit of infinite data with infinite order filtering; and the relation of filtering to the more familiar problem of “optimal” embedding.

II BLEACHING

Given a time series x_t , the best linear predictor \hat{x}_t is given by the model

$$\hat{x}_t = a_0 + \sum_{k=1}^q a_k x_{t-k} \quad (1)$$

for which \hat{x}_t most closely approximates x_t in the least-squares sense. The residuals (also called “innovations” or “disturbances”) $e_t = x_t - \hat{x}_t$ measure how much of the original time series is not linearly predictable from the past. That is,

$$e_t = x_t - \left[a_0 + \sum_{k=1}^q a_k x_{t-k} \right], \quad (2)$$

where q is the order of the model, and the linear coefficients a_k are obtained by a least-squares fit which minimizes the variance of the residuals.

A result from the theory of linear time series analysis states that in the large q limit, the residuals e_t obtained by subtracting from x_t the best linear predictor \hat{x}_t will be uncorrelated; that is, the residuals e_t are spectrally white (the Appendix outlines an informal proof).

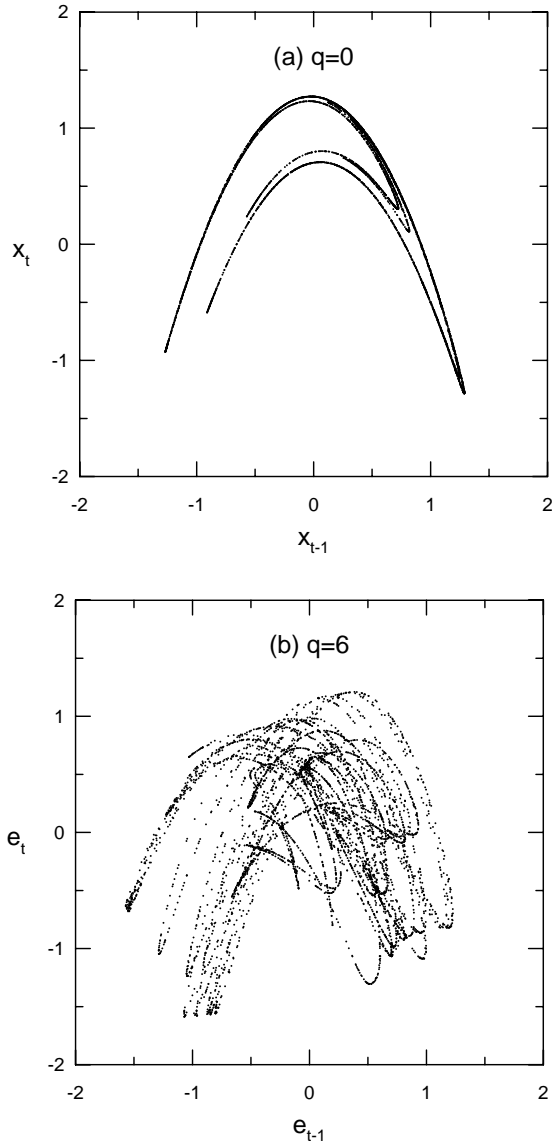


FIG. 1. Effect of bleaching on a time series derived from the x values of the Hénon map. (a) The unfiltered data corresponds to $q = 0$. (b) A $q = 6$ filter distorts the attractor considerably, and hides the determinism that is evident in the raw data.

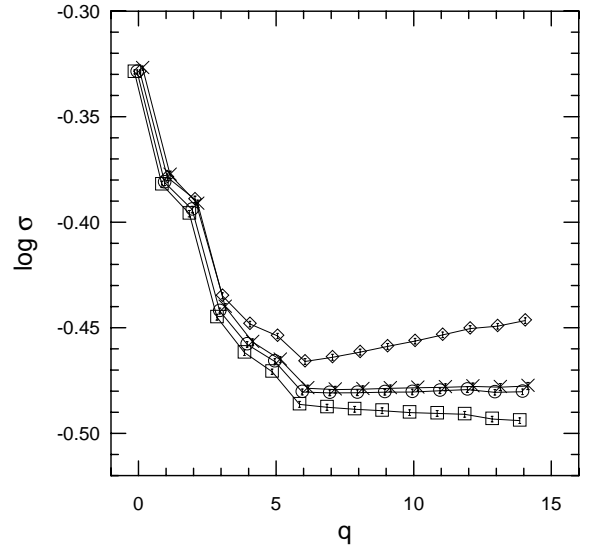


FIG. 2. Four measures of goodness of fit are plotted as a function of q for the Hénon map with $N = 1024$ points. The in-sample fitting error (\square) decreases monotonically with increasing q because there is no penalty for more parameters and no guard against overfitting. The out-of-sample fitting error (\times) and the Akaike Information Criterion (\circ) both show a leveling-off at $q = 6$, while the Schwarz criterion (\diamond) indicates a definite minimum at $q = 6$, suggesting that an order 6 fit is optimal with this many data points. The Akaike curve is $\log \sigma + q/N$ where σ is the in-sample rms fitting error, and the Schwarz curve is $\log \sigma + (q \log N)/2N$.

While the fit is based on the best auto-regressive (AR) *model*, the linear map that takes x_t to e_t in Eq. (2) is a moving-average (MA) *filter*; that is, it is a nonrecursive, finite order, or finite-impulse-response (FIR), filter. Strictly speaking, it will not change the structure of the attractor for finite q [6, 17–20]. For example, if x_t lies on a strange attractor, then e_t will lie on an attractor of the same dimension. This is not true of an AR filter, which can increase the dimension of the attractor [22, 23]. Actually, it *is* possible for a nongeneric MA filter to reduce the dimension, by “undoing” an AR filter’s increase [18, 19].

However, as Fig. 1 shows, the effect of bleaching the Hénon attractor [26] is to distort the attractor considerably, and to make its low-dimensionality much less evident. The order of the model, q , is generally chosen by some criterion which trades off the variance of the residuals (in-sample error of fit) against a penalty for number of parameters. In Fig. 2, we plot Akaike’s information criterion (AIC) [27], Schwarz’s criterion [28], and out-of-sample error as a function of q , and show that $q = 6$ is a good choice for the Hénon map with $N = 1024$ points.

III NONLINEAR MODELING

A very direct measure of determinism in a time series is the accuracy of a nonlinear predictor. We performed a numerical experiment that involved modeling the Hénon attractor with a nonlinear predictor based on local-linear fits to the k nearest neighbors [29]. The results are shown in Fig. 3. The time series contains $N = 1024$ points, half of which are used for learning the nonlinear map, and the other half for testing the goodness of the model. We used $k = 2m$, where m is the embedding dimension of the model. In general, increasing the embedding dimension (up to $m = 3$) im-

proves the prediction, but increasing q degrades the prediction. Nonlinear prediction of fully bleached data leads to errors that are in this case two orders of magnitude larger than errors obtained by directly fitting the raw data.

Note that for both the raw data and for the residuals, an embedding dimension of $m = 3$ is in principle adequate, since the fractal dimension is approximately $d \approx 1.3$ [30], and a theorem of Sauer *et al.* [17] states that as long as $m > 2d$, the embedding will almost always be sufficient.

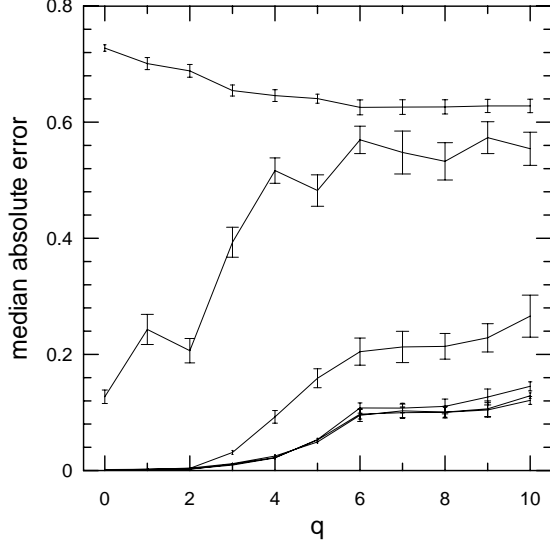


FIG. 3. Modeling error of a nonlinear predictor on a time series generated by the Hénon map. For $q = 0$, the raw data set is used. For $q > 0$, the q -th order residuals (as computed by Eq. (2)) are used. The top ($m = 0$) curve corresponds to the amplitude of the order- q residuals; these decrease with increasing q . The curve below that is from an $m = 1$ model, and below that is $m = 2$. The curves for $m = 3, 4, 5$ are essentially the same. (The error bars are based on five independent runs with different realizations of the data.)

We remark that fitting the residuals is different from a common two-step approach to fitting data that first fits a linear model, then fits a nonlinear model to what is left. To make this distinction clearer, let us write $\vec{x}_{t-1} = (x_{t-1}, \dots, x_{t-m})$. The best linear model to the time series is $\hat{x}_t = \mathcal{L}(\vec{x}_{t-1})$ with \mathcal{L} chosen to minimize the variance of the residuals $e_t = x_t - \mathcal{L}(\vec{x}_{t-1})$.

Nonlinear modeling of the residuals in terms of the actual past time series \vec{x}_{t-1} , that is

$$\hat{e}_t = \mathcal{N}(\vec{x}_{t-1}), \quad (3)$$

permits a full nonlinear model of the original time series: $\hat{x}_t = (\mathcal{L} + \mathcal{N})(\vec{x}_{t-1})$.

By contrast, nonlinear modeling of the bleached time series means finding a nonlinear map \mathcal{N}' which estimates e_t from past residuals \vec{e}_{t-1} .

$$\hat{e}_t = \mathcal{N}'(\vec{e}_{t-1}) \quad (4)$$

Combining \mathcal{L} and \mathcal{N}' into a full model for the original time series is possible, but far from natural. Furthermore, for chaotic data, we find that the estimation errors obtained with \mathcal{N}' are generally larger than those of the more direct \mathcal{N} .

Quasiperiodic data. The case against bleaching depends on the time series being chaotic. When applied to quasiperiodic data, the ill effects of bleaching are not evident.

For our numerical experiment, we deliberately chose an example that was more complicated than the sum of two sine waves. The quasiperiodic data were generated by a nonlinear two-frequency model with observational and dynamical noise:

$$x_t = \frac{X_{1,t} + X_{2,t} + 1}{X_{1,t}^2 + X_{2,t}^2 + 0.2} \quad (5)$$

where $X_{i,t} = \sin(\phi_i + (2\pi/5)\gamma_i t + \eta_{i,t}) + 0.1\varepsilon_{i,t}$. Here, the two mutually incommensurate frequencies are $\gamma_1 = (\sqrt{5} - 1)/2$ and $\gamma_2 = \sqrt{3} - 1$. Observational noise is modeled with ε , a Gaussian white noise process with unit variance; and dynamical noise is modeled as a random-walk phase drift: $\eta_t = \eta_{t-1} + 0.1\epsilon_t$, where ϵ_t is again Gaussian white noise with unit variance. Finally, ϕ is a randomly chosen initial phase. Five time series were generated, using different starting phases ϕ and a transient time $N_{\text{transient}} = 512$. The time series themselves were of length $N = 512$. Each was modeled by a local linear map with various embedding dimensions m and bleaching parameters q . We used the $k = 2m$ nearest neighbors from the first half of the data set for one-step-ahead predictions on the second half of the data set, and computed the median absolute error. As seen in Fig. 4, unlike the case with chaotic data, bleaching does not have such a debilitating effect on the modeling.

IV DETECTING NONLINEARITY

In this section, we will describe how bleaching influences statistical tests for nonlinearity. The motivation behind a test for nonlinearity is sometimes simply to determine whether a linear model will capture all of the structure in the time series. Often, however, there is a hidden agenda. One may seek to detect nonlinearity as a first step in what is ultimately a search for chaos. Nonlinearity is certainly a pre-requisite for chaos, but it is not the most straightforward way to test for chaos. A more direct approach might be to estimate the largest Lyapunov exponent. A positive Lyapunov exponent implies chaos, so a positive estimate would be taken as direct evidence in favor of chaos. The main problem with this approach is that the estimation of Lyapunov exponent is a nontrivial procedure [31, 32], and it is difficult to quantify the reliability of the estimate. Testing only for nonlinearity may not be as direct a test for chaos (the disadvantage being that a positive identification of nonlinearity does not imply chaos), but it can be done far more reliably than trying to compute a Lyapunov exponent.

Bleaching provides a conceptually simple approach to testing for nonlinearity in time series. Since the residuals of a bleached time series have no linear correlations, any correlations that are found in the residuals must be nonlinear. In particular, testing the residuals against IID (independent and identically distributed) is equivalent to testing the original time series for nonlinearity.

This is the basis of the Brock–Dechert–Sheinkman (BDS) test [5] (see Ref. [7] for a recent and more complete exposition), the tests for chaos described by Hsieh [9] (though with the financial time series of interest here, there is little autocorrelation to begin with [8]), a neural-net-based test for “neglected nonlinearity” [10], as well as a variety of classical nonlinearity tests [1, 2], many of which are reviewed in Tong [4]. To be fair, not all of these tests were designed with the idea of looking for chaos. Our point is that those tests which have bleaching as their first step will have low power when the test data is chaotic. We should also be careful to

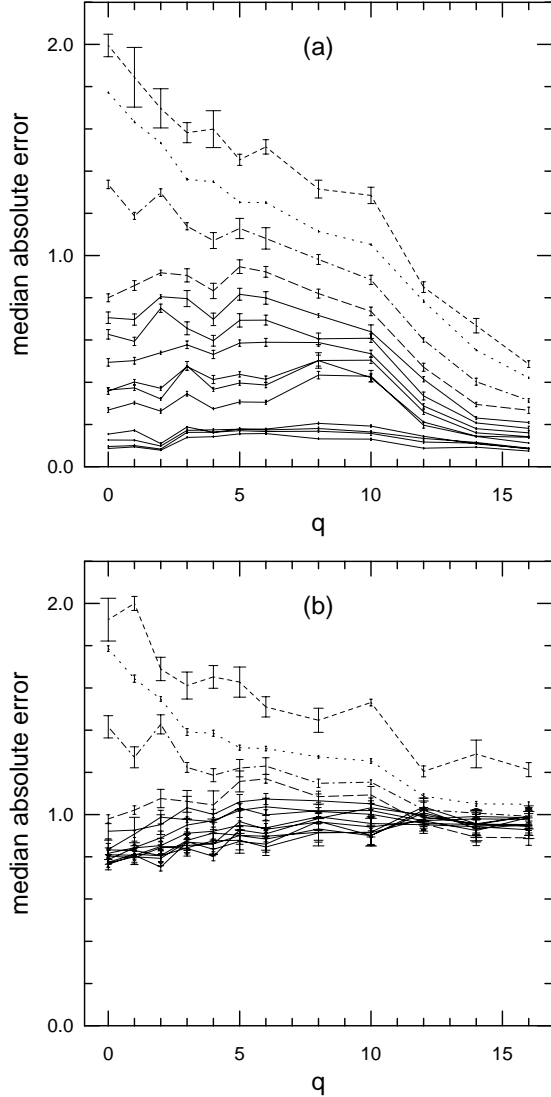


FIG. 4. Similar to Fig. 3, but instead of using chaotic data, we use (a) noise-free, and (b) noisy quasiperiodic data. Note that in contrast to the case of chaotic data, the effect of bleaching is not to degrade the accuracy of a nonlinear model, but on the contrary to improve it. Embedding dimensions shown are $m = 0$ (dotted line); $m = 1$ (short dashed line); $m = 2$ (dashed-dotted line); $m = 3$ (long dashed line); and $m = 4, 5, 6, 8, 10, 12, 14, 16, 18, 20$ (solid lines). In general, the larger the m , the smaller the error (except the $m = 0$ curve, which is actually more accurate than the $m = 1$ curve).

note that the test proposed by Tsay [3], though it involves residuals, also makes use of the original data. It has the flavor of Eq. (3) as opposed to Eq. (4), and unlike purely residual-based statistics, it may not suffer the same loss of power against chaotic time series.

Instead of comparing residuals to IID, a more direct approach is to compare the original data to surrogate data sets which mimic the linear correlations in the original time series, but which are otherwise random [25, 33–36]; in the statistical literature, the approach is often identified as a bootstrap. There is some discussion of the connection between the surrogate data approach and the classic bootstrap in Refs. [36, 37]; the interested reader should also consult Refs. [34, 38] for pointers into the relevant literature.

A discriminating statistic (which for chaotic processes is often chosen to be a dimension or Lyapunov exponent estimator, or the error in a nonlinear predictor, but in general can be any function that maps a full time series into a single number) is computed for each of the surrogates and for the original data set. If the number obtained for the original data set is significantly different from those obtained for the surrogate data sets, then a null hypothesis of linearly correlated noise can be rejected. A crude (and cheaply computed) measure of how significantly different the original is from the surrogate data is given by the number of “sigmas”:

$$\text{sigmas} = \frac{|\bar{Q}_{\text{surrogate}} - Q_{\text{original}}|}{\sigma_{\text{surrogate}}} \quad (6)$$

Here Q_{original} is the value of the discriminating statistic for the original data set, and $\bar{Q}_{\text{surrogate}}$ and $\sigma_{\text{surrogate}}$ are the mean and standard deviation, respectively, of the discriminating statistics computed for the surrogate data sets. We remark that this is a heuristic measure. Properly, one should compute the probability (also called the p -value) of mis-identifying a linear time series as nonlinear. One way to estimate p is from the percentile ranking of Q_{original} in a sorted list of all the Q values. Only when the Q statistic has a distribution of some previously assumed form (usually Gaussian) can the p -value can be computed directly from the number of sigmas. In general, though, the more sigmas, the smaller the p -value, and the more powerful the statistic. We will be using sigmas as an inexpensive measure of relative power.

Formally, the method of surrogate data provides a measure of statistical confidence that the null hypothesis is false; informally, it can be used as a control experiment to assess whether the measurement of a given nonlinear property is being fooled by simple linear correlation in the time series.

Our approach will be to compare the power of different tests for nonlinearity when the form of that nonlinearity is chaos. In statistical terminology, the null hypothesis is linearly correlated noise, and the alternative hypothesis is chaos. If the alternative hypothesis is a specific chaotic process, one can imagine designing very sensitive tests for distinguishing this process from the null. For the broad class of chaotic processes (and especially for the even broader class of nonlinear processes that may or may not be chaotic), the notion of an optimal design ceases to be well-posed. The emphasis here, however, will not be on finding the most powerful tests for nonlinearity; instead we will concentrate on the simpler question of how bleaching affects the power of existing tests when the alternative is chaos.

In the numerical experiment shown in Fig. 5, significance was computed for a variety of discriminating statistics on a chaotic time series and on time series obtained by bleaching with ever larger values of q . By and large, the significance was found to decrease with increasing q . We also performed some experiments with quasiperiodic data (not shown), and we found that bleaching

did not noticeably alter the ability of the surrogate data method to detect nonlinearity. We remark, however, that attempting to distinguish nonlinearity in quasiperiodic data is a very fussy issue. Stable limit cycles and limit tori arise only in nonlinear systems, yet the absence of chaos implies that linear models (of sufficiently high order) can in principle do as well as nonlinear models. This issue is discussed in further detail in Ref. [37].

In the method of surrogate data, just about any nonlinear statistic can be used. For example, we have found a very simple measure of nonlinearity that is motivated by the fact that linear time series have symmetric rise and fall times; the asymmetry in the derivative can be measured by a simple skew statistic, $\langle (x_t - x_{t-1})^3 \rangle$. For the experiment in Fig. 5, it is this statistic which we found most sensitive to the nonlinear structure in the time series. (See Tsay [34] for further discussion of this statistic.)

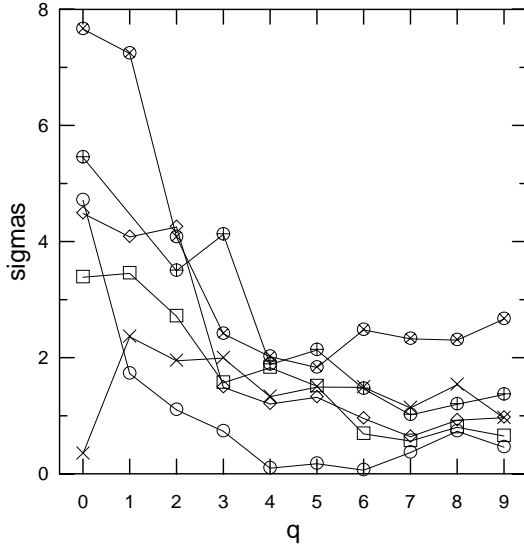


FIG. 5. Significance of rejection of a null hypothesis of linearly correlated noise versus bleaching parameter q for a variety of discriminating statistics: modified BDS (\oplus), a simple skew statistic (\otimes), estimated correlation dimension (\diamond), the correlation integral itself (\square), local linear forecasting error (\diamond), and modified McLeod-Li (\times). For the experiment in this figure, we used a time series of $N = 1024$ points obtained by summing four independent realizations of time series from the Hénon map. The dimension, BDS, and forecasting statistic used an embedding dimension of $m = 3$. Although this is clearly too small to see the full dynamics in the time series, for the purpose of finding evidence for nonlinearity from a series of this length, the value $m = 3$ was empirically found to give the most significance (the skew and modified McLeod-Li statistics do not require an embedding). All of the discriminating statistics (except the modified McLeod-Li) show evidence of nonlinearity at the three sigma level for unbleached data ($q = 0$), and all of them *fail* to show evidence of nonlinearity at the three sigma level for the fully bleached data ($q \geq 6$).

IV.A COMPARISON TO BDS

Brock, Dechert, and Scheinkman [5] developed a statistic to test for nonlinearity based on the correlation integral of Grassberger and Procaccia [39]. This is, to our knowledge, the first statistically rigorous test to exploit the “new paradigm” of deterministic chaos

as an alternative hypothesis. To define the BDS statistic for a time series of N points, first define $C_m(N, r)$ as the m -dimensional correlation integral

$$C_m(N, r) = \frac{2}{N(N-1)} \sum_{i=1}^N \sum_{j=1}^{i-1} \prod_{k=0}^{m-1} \Theta(r - |x_{i+k} - x_{j+k}|) \quad (7)$$

where $\Theta(x)$ is the Heaviside step function; it is one for positive x , and zero otherwise. For IID data, in the limit $N \rightarrow \infty$, one expects $C_m(N, r) \approx C_1(N, r)^m$. In particular, the BDS statistic

$$Q_{\text{BDS}} = \sqrt{N} [C_m(N, r) - C_1(N, r)^m] \quad (8)$$

will for IID data converge to a normal distribution with zero mean and fixed variance. The variance can be estimated from the data, but for our purposes, we find it convenient to estimate the variance using Monte-Carlo simulation.

In particular, we use Q_{BDS} as the discriminating statistic in the scheme of surrogate data. We find that as a discriminating statistic, it is quite powerful. However, when it is applied to bleached data, it loses its original power. We suggest therefore that the BDS statistic should not be applied to residuals and compared against IID, but instead should be applied to the original data and compared against the appropriate surrogates (see Fig. 6).

IV.B COMPARISON TO MCLEOD-LI

One of the most straightforward conventional approaches to testing for linearity in a time series is to look at the autocorrelation of the squared residuals. If the residuals truly are IID, then their squares will be IID, and therefore, the squares will have zero autocorrelation. In particular, the statistic based on sample autocorrelation of the squares

$$Q_{\text{ML}} = N(N+2) \sum_{k=1}^m \frac{1}{N-k} r_k^2, \quad (9)$$

where

$$r_k = \frac{\langle e_t^2 e_{t-k}^2 \rangle - \langle e_t^2 \rangle^2}{\langle e_t^4 \rangle - \langle e_t^2 \rangle^2} \quad (10)$$

is the autocorrelation of the squared time series, will for IID data converge as $N \rightarrow \infty$ to a well-defined distribution. This is a particular case of the McLeod-Li [1] statistic [40]. As in the case of the BDS statistic, we can apply the statistic to unbleached data by simply using $x_t - \langle x_t \rangle$ in place of e_t in the above formula. However, at least for the numerical experiment in Fig. 5, we found that this statistic was the weakest of our tests for nonlinearity.

Further, the McLeod-Li statistic seems to *improve* when the data set is bleached. This can be understood intuitively by realizing that the autocorrelation of the squared time series involves very large values (and therefore, very large variances). One natural way to reduce these values is with the following modification:

$$Q_{\text{MML}} = N(N+2) \sum_{k=1}^m \frac{1}{N-k} (r_k - A_k^2)^2 \quad (11)$$

where r_k is the autocorrelation in the squared time series (as before), and A_k is the autocorrelation of the original time series.

$$A_k = \frac{\langle x_t x_{t-k} \rangle - \langle x_t \rangle^2}{\langle x_t^2 \rangle - \langle x_t \rangle^2}. \quad (12)$$

The idea is to “subtract off” that much of the autocorrelation of the squares which can be attributed to the autocorrelation in the original time series. Fig. 7 shows that the new statistic is more powerful when used with surrogate data; and for the data set under consideration, is optimal for a small value of q .

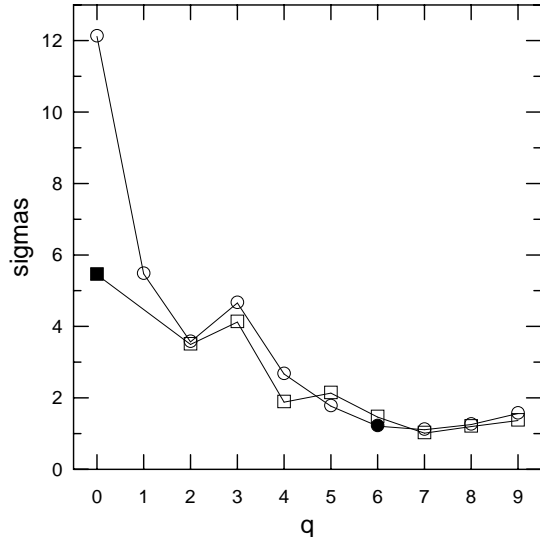


FIG. 6. Significance of the BDS statistic as a function of bleaching q . The time series is $N = 1024$ points obtained by adding four independent realizations of Hénon time series. As with the single Hénon time series, full bleaching occurs at $q = 6$. The circle (○) curve uses BDS to test against a null of IID noise. Not surprisingly, the null is easily rejected for unbleached data, because there are both linear and nonlinear correlations, and the test doesn't distinguish them. However, applying the test to bleached data, we find little evidence to reject the null of IID residuals. On the other hand, the square (□) curve uses the BDS statistic as part of a surrogate data algorithm to test directly against the null hypothesis of linearly correlated noise. This test is less significant at $q = 0$, but that's because it is testing against a more general null. It too loses significance as q increases. But what should be compared here is the $q = 0$ square (■) point, and the $q = 6$ circle (●) point; the former is significant at the five sigma level, while the latter is not significant. The former uses the BDS to test the raw time series against a null of linearly correlated noise; the latter uses BDS (as it was originally intended) to test residuals against IID; though the two tests are formally equivalent, the direct test that avoids bleaching is the more powerful.

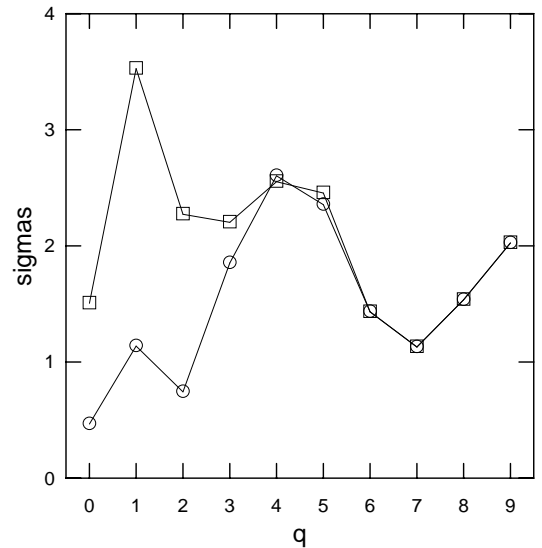


FIG. 7. Significance of nonlinearity for a time series of $N = 1024$ points obtained by summing four realizations of the Hénon map, using the McLeod-Li statistic (○) and a modified version of McLeod-Li (□) described in Eq. (11).

V SOME GENERAL REMARKS ON LINEAR FILTERING

In the case of the Hénon attractor, bleaching is found to be detrimental both to nonlinear modeling and to detecting nonlinearity. But it would be incorrect to assume that all linear filtering is in all cases bad. Given a particular data set, and a particular nonlinear task, one expects that there is a particular linear prefiltering that will optimize the performance at the given task. The theme of this article is that the particular linear filter that corresponds to bleaching is rarely optimal, and usually makes things worse.

In this section, we will give two examples of situations that arise frequently in practice. In both cases, linear prefiltering is seen to be advantageous, but in neither case is *full* bleaching recommended.

V.A UNFILTERING FILTERED DATA

A natural example is to begin with a known chaotic time series, and then to low-pass filter the data, so as to introduce a lot of linear correlation in the data. For example, if h_t is a chaotic time series, and $|\alpha| < 1$, then

$$x_t = \alpha x_{t-1} + h_t \quad (13)$$

gives a time series x_t which for α near 1 is dominated by the linear component [41]. While this example may appear at first sight contrived, it represents a very common physical occurrence: the observation of a natural phenomenon through a low-pass filter. For instance, a resistance R and capacitance C between the probe and the phenomenon being measured leads to a characteristic time of RC , and corresponds to $\alpha = e^{-1/RC}$ in Eq. (13). This is certainly the situation for the example of scalp-based measurements of brain electrical activity, as in the electroencephalogram (EEG).

In this case, it can be advantageous to digitally filter the observed time series to counteract the effect of the filter through which the data were observed. However, it is *still* not recommended to fully bleach the data! In particular, Fig. 8 shows that for a sum of four Hénon time series, prefiltered with $\alpha = 0.9$, the optimum amount of bleaching is given at $q = 1$ or 2. However, from the point of view of linear modeling, $q = 7$ is the “proper” amount of

bleaching for this time series (based, as in Fig. 2, on AIC, Schwartz, and out-of-sample error criteria). At $q = 7$, the significance of the evidence for nonlinearity is negligible. The evidence at $q = 0$ is not very significant (depending on the discriminating statistic), so there is a real advantage to a “little” bleaching to remove a dominating linear component.

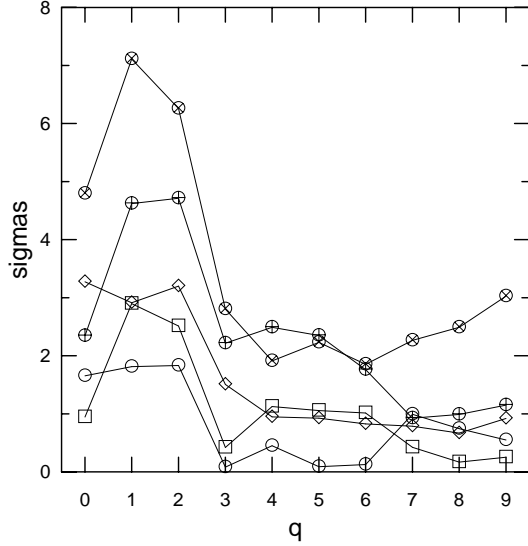


FIG. 8. Here, the chaotic time series is obtained by AR filtering ($a = 0.9$) a time series of four independent Hénon maps summed together. The time series is bleached at several values of q . As before, the embedding dimension is $m = 3$. Some bleaching (at $q = 1$ or 2) leads to significant evidence for nonlinearity, but full bleaching (at $q = 7$ for this time series) gives time series with no detectable nonlinear structure. Here, the discriminating statistics used were: modified BDS (\oplus), skew (\otimes), correlation dimension (\circ), correlation integral (\square), and local linear forecasting error (\diamond).

In a more practical situation, if one is seeking evidence for nonlinearity in a time series of sea levels, it can be advantageous to “filter out” the daily and monthly tides which dominate the variations [42]. We also note that Townshend [43] reported improved modeling of speech signals after linear filtering; we suspect that this is due to the dominant underlying periodicity of these signals.

V.B BLEACHING OVERSAMPLED DATA

Data which are sampled at a much higher rate than that of the underlying physical process will have very little power in the high frequencies. Since the effect of bleaching is to achieve equal power at all frequencies, the effect on oversampled data is to grossly amplify the high frequency behavior.

For noise-free oversampled data, the residuals will have very small amplitude compared to the original data, but the enhancement of the high frequencies will lead to very irregular and “spiky” dynamics. Fig. 9 shows this effect with the Lorenz attractor [44]; data from the Rossler attractor [45], which has a more pronounced periodicity, shows the effect even more severely.

For a time series which is oversampled from a continuous flow but whose measurement is contaminated with uncorrelated additive noise, the effect of bleaching is to amplify the noise. Because this situation is so common in physics experiments, it is sometimes difficult for physicists to imagine why one would ever want

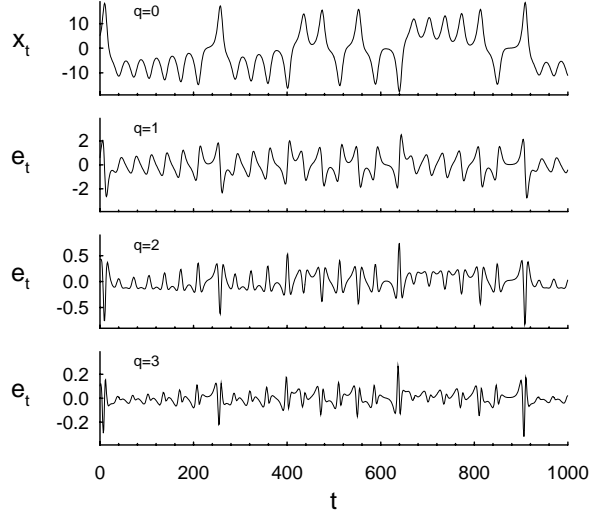


FIG. 9. Bleaching oversampled data; the Lorenz time series was sampled at a rate $\Delta t = 0.02$, and residuals were computed for $q = 1, 2, 3$. While bleaching significantly reduced the magnitude of the residuals, it produced in its place a very “spiky” time series that is more difficult to analyze than the raw data.

to bleach data in the first place. The physicist’s intuition in this case is absolutely correct. This is an example where it is not only unwise to bleach the data, but it is often helpful to filter the data with a low-pass filter, making it *less white* than the original signal.

VI THEORETICAL CONSIDERATIONS

We have emphasized numerical experiments in this exposition, partly because these provide graphic demonstrations of the phenomena, but also because we do not have a good “theory” of why bleaching should be so detrimental to so many different aspects of nonlinear time series analysis. Intuitively, the linear filtering replaces the current state with a linear combination of states at previous times, and the effect of this combination is to confuse the meaning of the current state; this intuition is made more precise in the following section.

VI.A LIMIT OF INFINITE DATA

When an infinite amount of data is available, then conditions such as those plotted in Fig. 2 do not put a cap on the order of the bleaching filter. That is, one may have $q \rightarrow \infty$ in Eq. (2). This is no longer a finite-impulse-response (FIR) filter, but is an infinite-impulse-response (IIR) filter, and so the theorems of Refs. [6, 17–20] no longer apply. The filtered time series is no longer guaranteed to preserve the nonlinear invariants, such as attractor dimension, of the original time series. In this section, we describe conditions under which a particular invariant, the Lyapunov dimension, is altered. We speculate that these conditions will apply to more general invariants as well.

The Lyapunov dimension was defined by Kaplan and Yorke [46] as part of a conjecture that related Lyapunov exponents to fractal dimension. If $\lambda_1 \geq \lambda_2 \geq \dots$ are the ordered Lyapunov exponents of a dynamical system, and k is the largest integer such that $\lambda_1 + \dots + \lambda_k > 0$, then the Lyapunov dimension is given by

$$D_\lambda = k + \frac{\lambda_1 + \dots + \lambda_k}{|\lambda_{k+1}|}. \quad (14)$$

Note that the Lyapunov dimension depends only on the largest $k + 1$ Lyapunov exponents.

The effect of a general (causal [47]) IIR filter is to add new negative Lyapunov exponents to the dynamics. This is readily seen in the case of the AR(1) filter. As discussed by Badii *et al.* [22], the filter

$$e_t = be_{t-1} + x_t \quad (15)$$

adds a new variable (e_t) to the dynamical system, and a new Lyapunov exponent $\lambda = \log |b|$. A higher order AR(q) filter

$$e_t = \sum_{k=1}^q b_k e_{t-k} + x_t \quad (16)$$

can be factored to give q new variables, and q new Lyapunov exponents. If z_1, \dots, z_q denote the q roots of the associated polynomial $Q(z) = 1 - \sum_{i=1}^q b_i z^i = (1 - z/z_1) \cdots (1 - z/z_q)$, then we can write Eq. (16) as a system of q equations:

$$\begin{aligned} e_t^{(1)} &= (1/z_1)e_{t-1}^{(1)} + e_t^{(2)} \\ &\vdots \\ e_t^{(q)} &= (1/z_q)e_{t-1}^{(q)} + x_t \end{aligned} \quad (17)$$

and the new Lyapunov exponents are given by $\lambda_i = \log(|1/z_i|) = -\log |z_i|$ for $i = 1, \dots, q$. Note that the roots z_i must all lie outside the unit circle ($|z_i| > 1$) for the filter in Eq. (16) to be stable, and in this case all the new Lyapunov exponents are negative.

If we rewrite the AR(q) filter above in terms of its equivalent MA(∞) filter; that is,

$$e_t = \sum_{k=0}^{\infty} a_k x_{t-k}, \quad (18)$$

then the polynomial

$$P(z) = \sum_{k=0}^{\infty} a_k z^k \quad (19)$$

will satisfy $P(z) = 1/Q(z)$ and will have poles z_1, \dots, z_q where $Q(z)$ has roots.

All of this is motivation for the following statements: The new Lyapunov exponents generated by an IIR filter given in Eq. (18) are $\lambda_i = -\log |z_i|$ where z_i are the poles of the polynomial in Eq. (19). If the filter is invertible and has bounded coefficients a_k , then there will be no poles or zeros inside the unit circle.

Now, we wish to consider the particular IIR filter that corresponds to bleaching. This is given by Eq. (2) with $q = \infty$, and has the property

$$\langle e_t e_{t-\tau} \rangle = \sigma^2 \delta_{0,\tau}. \quad (20)$$

Let us write the causal inverse of the filter in Eq. (2) as

$$x_t = \sum_{k=0}^{\infty} b_k e_{t-k} \quad (21)$$

where the b 's are given as the coefficients of the polynomial

$$Q(z) = \sum_{k=0}^{\infty} b_k z^k = \frac{1}{P(z)}. \quad (22)$$

We can exploit the condition in Eq. (20) by writing

$$\begin{aligned} \langle x_t x_{t+k} \rangle &= \sum_{i=0}^{\infty} \sum_{j=0}^{\infty} b_i b_j \langle e_{t-i} e_{t+k-j} \rangle \\ &= \sigma^2 \sum_{i=0}^{\infty} b_i b_{i+k}. \end{aligned} \quad (23)$$

If we introduce the autocorrelation “generating function” (Ref. [48], Sec. 5.7.1) which is the polynomial

$$\mathcal{A}(z) = \sum_{k=-\infty}^{\infty} A_k z^k \quad (24)$$

where A_k is the autocorrelation function defined in Eq. (12), it is not hard to show that

$$\mathcal{A}(z) = cQ(z)Q(z^{-1}) \quad (25)$$

where c is a constant multiplier. Thus, if z_o is a root of $Q(z)$, then both z_o and z_o^{-1} are roots of $\mathcal{A}(z)$. It follows that the largest new Lyapunov exponent introduced by the bleaching is given by

$$\lambda_o = -\log |z_o| \quad (26)$$

where z_o is the smallest root of the autocorrelation generating function $\mathcal{A}(z)$ that is *outside* the unit circle.

Since the Lyapunov dimension D_λ depends only on the largest D Lyapunov exponents, where $D = \lceil D_\lambda \rceil$, a new Lyapunov exponent will change the Lyapunov dimension only if it is larger than λ_D , the D th largest Lyapunov exponent of the original dynamics. These D largest Lyapunov exponents are the only ones accessible from a trajectory that is on the attractor; Čenys [49] calls these the “internal” Lyapunov exponents.

Therefore, a bleaching filter will change the Lyapunov dimension whenever λ_o of Eq. (26) is greater than the smallest accessible (or “internal”) Lyapunov exponent λ_D . One can think of this in terms of two time scales: one is the “linear” timescale associated with the autocorrelation function, and the other is the “nonlinear” timescale associated with the smallest accessible Lyapunov exponent. When the linear timescale is longer than the nonlinear timescale, then bleaching will, in the infinite data limit, actually change the structure of the attractor.

We have already seen, however, that even finite-order bleaching can have a dramatic effect on estimates of nonlinear invariants, and in the following section we outline an approach for quantifying that effect.

VI.B FILTERING, EMBEDDING, AND PROJECTING

As noted in Refs. [17–19], the issue of prefiltering can be recast as an embedding problem. Given a time series x_t , one can ask which of the following “embeddings” best describes the actual state of the system at time t :

$$\begin{aligned} S_t^{(0)} &= (x_t, x_{t-1}, x_{t-2}); \text{ or} \\ S_t^{(a)} &= (e_t, e_{t-1}, e_{t-2}) \\ &= (x_t - ax_{t-1}, x_{t-1} - ax_{t-2}, x_{t-2} - ax_{t-3}). \end{aligned} \quad (27)$$

And in fact, *both* of these are projections from the higher dimensional space: $(x_t, x_{t-1}, x_{t-2}, x_{t-3})$. Indeed, the two panels in Fig. 1 can be viewed as two different projections from the eight-dimensional space $(x_t, x_{t-1}, \dots, x_{t-7})$. Thus the twin issues of

optimal filtering and optimal embedding can both be rephrased in terms of optimal projection.

There are a number of criteria for judging the quality of an embedding. Operational criteria would define the fitness of an embedding in terms of how well it permits nonlinear forecasting or dimension estimation. More direct criteria have also been proposed [50–53].

In particular, the approach suggested by Casdagli *et al.* [50] compares different embeddings according to how measurement noise is amplified when the embedded state is mapped back to the original state space. The authors define a “distortion” δ which is related to this amplification. In this section, we will measure δ for bleached and unbleached data. We will also introduce a new quantity, γ , which we will call “stretching;” this measures how much a spherical (infinitesimal) noise ball in the original state space will be stretched in going to the embedded space. This new quantity, though also a local quantity (by which we mean it does not depend on global information in the attractor, such as how the attractor is “folded” by the dynamics), provides complimentary information about the embedding.

Following Casdagli *et al.* [50], let Φ be the map that takes the actual state into the time delay embedding: $\Phi : \mathbf{R}^d \rightarrow \mathbf{R}^{m+q}$, where d is the dimension of the actual state space. Let Ψ_T and Ψ_B denote two different projections of the time delay embedding from $m+q$ coordinates to m coordinates. Ψ_T is just the map that projects out the first m coordinates, and Ψ_B is the projection that corresponds to bleaching the time series. Let $D\Phi$ and $D\Psi$ be the Jacobians of these maps; in general they will depend on the location in state space.

From $D\Phi$ and $D\Psi$, a “distortion” matrix can be defined [50, Eq. (75)]

$$\Sigma = [D\Phi^T D\Psi^T (D\Psi D\Psi^T)^{-1} D\Psi D\Phi]^{-1} \quad (29)$$

and the distortion itself is given by $\delta = \sqrt{\text{Trace}(\Sigma)}$. Casdagli *et al.* [50] have noted that if Ψ is invertible, there will be no effect at all on distortion. However, even if the *filter* is invertible, the matrix Ψ is still a projection, and it is *not* invertible.

We define the stretching matrix simply as the inverse of the distortion matrix, and so the stretching itself is $\gamma = \sqrt{\text{Trace}(\Sigma^{-1})}$. Note that while the distortion is sensitive to large eigenvalues of Σ , the stretching is sensitive to small eigenvalues of Σ . A more comprehensive theory might consider the full eigenvalue spectrum. Note also, in comparison with Eq. (83) of Ref. [50], that this is a local quantity that appears related to estimation error.

In Fig. 10, we compare the distortion for the embeddings of a Hénon time series bleached at increasing levels of q . We again remark that an embedding dimension of $m = 3$ is sufficient for all finite values of q because the Hénon attractor has a dimension $d \approx 1.3$, and $m > 2d$. It appears from these figures that bleaching does not induce considerable distortion, but that it does a phenomenal amount of stretching.

Another way of looking at what is happening can be seen in Fig. 11. Here, distances between pairs of residuals ($\Delta e_{ij} = |\vec{e}_i - \vec{e}_j|$) are plotted as a scatterplot against the corresponding distances for the original time series ($\Delta x_{ij} = |\vec{x}_i - \vec{x}_j|$). Again, we use an embedding dimension of $m=3$, so that the attractors do not overlap themselves. We see a large population of points for which $\Delta e \gg \Delta x$; these are pairs of points which are close in the original coordinates, but have been stretched far apart in the residual coordinates.

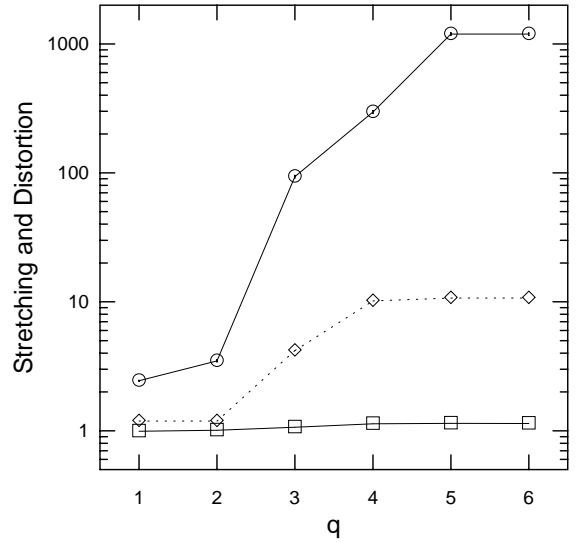


FIG. 10. Mean (□) and maximum (◇) distortion, and mean stretching (○) as a function of bleaching order q , for an $m = 3$ embedding of the Hénon time series. The effect of bleaching on distortion is quite small; on average it is very near unity, and at the few points where the effect is maximal, it is only of order ten. The average stretching, by contrast (compare circles (○) with squares (□)), increases dramatically with q .

VII CONCLUDING REMARKS

In a variety of numerical experiments, we have described the ill effects of bleaching on nonlinear models of chaotic time series data. We have shown in particular that for detecting nonlinearity, it is often better to compare the given time series with stochastic data that mimics its autocorrelation than to try and subtract out the autocorrelation altogether. This led us to suggest modifications to some standard residual-based statistics, among them the BDS and the McLeod-Li statistics. From the point of view of model building, we have seen that fitting of residuals can cost several orders of magnitude in accuracy of fit, compared to fitting the original data. On the other hand, having demonstrated cases where linear prefiltering is disadvantageous, we have also seen cases where *some* linear filtering helps.

We have also done experiments with the correlation dimension, and while these results are not shown (but see Sauer and Yorke [19] for a demonstration of how linear filtering can affect estimates of correlation dimension), these estimates are also seriously degraded by the effects of bleaching. Although we have not done the relevant numerical experiments, we suspect that indiscriminate bleaching will have a similarly deleterious effect on estimates of Lyapunov exponent, or upon the tests for determinism advocated by Casdagli [54] and Kaplan [55].

Brock [6] has noted that residual-based statistics “may misidentify deterministic chaos as random noise in a short data set,” but chose to use a residual-based statistic in his study for reasons that were to some extent motivated by the considerable interest at the time in AR(2) models with roots near the unit circle [56]; for such systems, as we noted in Sect. V.A, pre-whitening can help. More recent modeling by Brock *et al.* [57] used a direct resampling (surrogate data) method for rejecting a variety of null hypotheses. While these conclusions suggest that earlier failures to detect nonlinearity in various economic time series may be vulnerable to

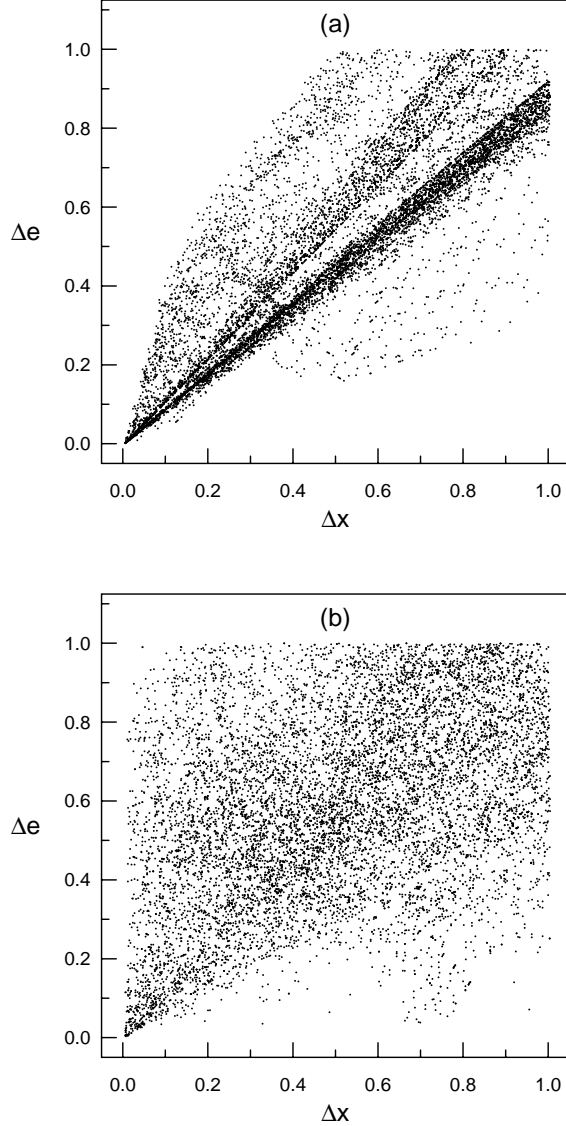


FIG. 11. The distance between a pair of points in the residual embedding (Δe) is plotted against the distance between the same pair of points in the original space (Δx). Note that there are many points for which the distance in the residual embedding space is much larger than the corresponding distance in the original embedding, *i.e.*, $\Delta e \gg \Delta x$. There are relatively fewer points for which $\Delta e \ll \Delta x$, which suggests that stretching, and not distortion, is the dominant factor in this case. The time series is from the Hénon map and the embedding dimension is $m = 3$. (a) Only a single bleaching term, $q = 1$. (b) Full bleaching, $q = 6$.

more powerful tests that are not based on residuals, we consider this unlikely, because our tests are more powerful when the alternative hypothesis is chaos, and we have seen no convincing evidence of chaos in financial time series. On the other hand, we are saying that if chaos is the alternative hypothesis, then residual based statistics are probably not as powerful as direct comparisons with similarly autocorrelated (surrogate) data.

Scargle [58] has suggested that a kind of nonlinear Wold decomposition theorem can be derived in which the chaotic process is rewritten as a linear filter of “white chaos.” This uncorrelated process is just the residual time series e_t of Eq. (2), and our main point in this article is that the residual time series can be much more complicated and difficult to work with than the raw time series. White chaos pays a price for its whiteness. Actually, the algorithm Scargle used for determining the chaotic innovation was more complicated than that of Eq. (2), and in a later paper [59], he recognizes that this algorithm does not in general produce a time series that is in fact uncorrelated. We do not know if the effective prefilter that Scargle ultimately proposes is in general beneficial or detrimental to nonlinear modeling of the time series.

Sugihara and May [60] have noted that their test for chaos based on prediction error can be fooled by autocorrelated noise, and they suggest first-differencing as a method of removing autocorrelation. Although this may be useful in some cases, we argue that this general approach is likely to be problematic on several counts. One, first differencing does not necessarily remove autocorrelation, and in some cases can enhance it; two, in cases where autocorrelation is not removed, the test is still vulnerable to linear artifacts; and three, even if the autocorrelation is significantly removed, the state space structure can become significantly distorted, and the power of the test for detecting nonlinearity (let alone chaos) will have been compromised.

APPENDIX: DEMONSTRATION THAT BEST FIT RESIDUALS ARE WHITE

In this appendix, we show that in the limit $q \rightarrow \infty$, the best linear fit leads to uncorrelated residuals.

Let \hat{x}_t be the “best” linear estimator for x_t , in the sense of minimizing the variance $\langle e_t^2 \rangle$ of the residuals, where $e_t = x_t - \hat{x}_t$. Consider an arbitrary time delay $\tau > 0$, and let

$$\lambda = \frac{\langle e_t e_{t-\tau} \rangle}{\langle e_t^2 \rangle}. \quad (30)$$

Since we want to show that the residuals are uncorrelated, what we want to show is that $\lambda = 0$. Our approach will be to show that if $\lambda \neq 0$, then a better linear estimator than \hat{x}_t can be constructed, contradicting the hypothesis that \hat{x}_t was optimal.

Begin by noting that a good estimator for e_t is given by

$$\hat{e}_t = \lambda e_{t-\tau} \quad (31)$$

so that a new linear estimator for x_t can be defined by

$$\begin{aligned} \hat{\hat{x}}_t &= \hat{x}_t + \hat{e}_t \\ &= \hat{x}_t + \lambda(x_{t-\tau} - \hat{x}_{t-\tau}). \end{aligned} \quad (32)$$

Note that this too is an ordinary linear estimator for x_t in terms of past values (x_{t-1}, \dots) . Note also, that if \hat{x} were restricted to finite order q , then $\hat{\hat{x}}$ would be of order $\tau + q$, so this argument does not apply to finite estimators, except through a separate result which we will not show here (see, for instance, Theorem 7.6.6 in Anderson [48]) that finite-order estimators approximate infinite-order estimators as $q \rightarrow \infty$.

Let ϵ_t be the residuals from this new estimator: $\epsilon_t = x_t - \hat{x}_t$. Then

$$\begin{aligned}
\langle \epsilon_t^2 \rangle &= \langle (x_t - \hat{x}_t)^2 \rangle \\
&= \langle (x_t - [\hat{x}_t + \hat{\epsilon}_t])^2 \rangle \\
&= \langle ([x_t - \hat{x}_t] - \hat{\epsilon}_t)^2 \rangle \\
&= \langle (e_t - \lambda e_{t-\tau})^2 \rangle \\
&= \langle e_t^2 \rangle - 2\lambda \langle e_t e_{t-\tau} \rangle + \lambda^2 \langle e_{t-\tau}^2 \rangle \\
&= (1 - \lambda^2) \langle e_t^2 \rangle.
\end{aligned} \tag{33}$$

From our original hypothesis that \hat{x} was the optimum linear predictor, we have $\langle e_t^2 \rangle \leq \langle \epsilon_t^2 \rangle$, which requires $\lambda = 0$, and implies that $\langle e_t e_{t-\tau} \rangle$ is zero for all $\tau > 0$. That is, the residuals have no autocorrelation; they are white.

ACKNOWLEDGEMENTS

We are pleased to acknowledge Bryan Galdrikian, André Longtin, and Doyné Farmer, who collaborated with us in developing the method of surrogate data. We are also grateful to Blake LeBaron, William Brock, Tim Sauer, and Lou Pecora for many useful discussions. This work was partially supported by the National Institute for Mental Health under Grant No. 1-R01-MH47184, and performed under the auspices of the U.S. Department of Energy.

REFERENCES

1. A. I. McLeod and W. K. Li, "Diagnostic checking ARMA time series models using squared-residual autocorrelations," *J. Time Series Anal.* **4**, 269–273 (1983).
2. D. M. Keenan, "A Tukey nonadditivity-type test for time series nonlinearity," *Biometrika* **72**, 39–44 (1985).
3. R. S. Tsay, "Nonlinearity tests for time series," *Biometrika* **73**, 461–466 (1986).
4. H. Tong, *Non-linear Time Series: A Dynamical System Approach*. (Clarendon Press, Oxford, 1990).
5. W. A. Brock, W. D. Dechert, and J. Scheinkman, "A test for independence based on the correlation dimension," Technical Report 8702, Social Systems Research Institute, University of Wisconsin, Madison (1987).
6. W. A. Brock, "Distinguishing random and deterministic systems," *J. Econ. Theo.* **40**, 168–195 (1986).
7. W. A. Brock, D. A. Hsieh, and B. LeBaron, *Nonlinear Dynamics, Chaos, and Instability: Statistical Theory and Economic Evidence*. (MIT Press, Cambridge, MA, 1991).
8. D. A. Hsieh, "Testing for nonlinear dependence in daily foreign exchange rate changes," *J. Business* **62**, 339–368 (1989).
9. D. A. Hsieh, "Chaos and nonlinear dynamics: application to financial markets," *J. Finance* **46**, 1839–1877 (1991).
10. T.-H. Lee, H. White, and C. W. J. Granger, "Testing for neglected nonlinearity in time series models: A comparison of neural network methods and alternative tests," *J. Econometrics* **56**, 269–290 (1993).
11. R. B. Blackman and J. W. Tukey, *The Measurement of Power Spectra*. (Dover, New York, 1959).
12. J. Theiler, "Spurious dimension from correlation algorithms applied to limited time series data," *Phys. Rev. A* **34**, 2427–2432 (1986).
13. A. R. Osborne and A. Provenzale, "Finite correlation dimension for stochastic systems with power-law spectra," *Physica D* **35**, 357–381 (1989).
14. A. Provenzale, A. R. Osborne, and R. Soj, "Convergence of the K_2 entropy for random noises with power law spectra," *Physica D* **47**, 361–372 (1991).
15. J. Theiler, "Some comments on the correlation dimension of $1/f^\alpha$ noise," *Phys. Lett. A* **155**, 480–493 (1991).
16. P. E. Rapp, A. M. Albano, T. I. Schmah, and L. A. Farwell, "Filtered noise can mimic low dimensional chaotic attractors," *Phys. Rev. E* **47**, 2289–2297 (1993).

17. T. Sauer, J. A. Yorke, and M. Casdagli, "Embedology," *J. Stat. Phys.* **65**, 579–616 (1991).
18. D. S. Broomhead, J. P. Huke, and M. R. Muldoon, "Linear filters and nonlinear systems," *J. R. Stat. Soc. B* **54**, 373–382 (1992).
19. T. Sauer and J. A. Yorke, "How many delay coordinates do you need?" *Int. J. Bifurcation Chaos* (1993). To appear.
20. S. H. Isabelle, A. V. Oppenheim, and G. W. Wornell, "Effects of convolution on chaotic signals." Preprint, MIT Research Laboratory of Electronics.
21. L. M. Pecora and T. L. Carroll, "Attractor reconstruction, filtering, and ill-posed problems." Preprint, Naval Research Laboratory.
22. R. Badii, G. Broggi, B. Derighetti, M. Ravani, S. Ciliberto, A. Politi, and M. A. Rubio, "Dimension increase in filtered chaotic signals," *Phys. Rev. Lett.* **60**, 979 (1988).
23. F. Mitschke, M. Möller, and W. Lange, "Measuring filtered chaotic signals," *Phys. Rev. A* **37**, 4518–4521 (1988).
24. F. Mitschke, "Acausal filters for chaotic signals," *Phys. Rev. A* **41**, 1169–1171 (1990).
25. J. Theiler, B. Galdrikian, A. Longtin, S. Eubank, and J. D. Farmer, "Using surrogate data to detect nonlinearity in time series," in *Non-linear Modeling and Forecasting. Proceedings of the Workshop held September, 1990, in Santa Fe, New Mexico*, M. Casdagli and S. Eubank, eds. Vol. XII of *SFI Studies in the Sciences of Complexity*, (Addison-Wesley, 1992), pp. 163–188.
26. M. Hénon, "A two-dimensional mapping with a strange attractor," *Comm. Math. Phys.* **50**, 69–77 (1976).
27. H. Akaike, "A new look at the statistical model identification," *IEEE Trans. Auto. Control* **19**, 716–723 (1974).
28. G. Schwarz, "Estimating the dimension of a model," *Ann. Stat.* **6**, 461–464 (1978).
29. J. D. Farmer and J. J. Sidorowich, "Predicting chaotic time series," *Phys. Rev. Lett.* **59**, 845–848 (1987).
30. P. Grassberger, "On the fractal dimension of the Hénon attractor," *Phys. Lett. A* **97**, 224–226 (1983).
31. H. D. I. Abarbanel, R. Brown, and M. B. Kennel, "Lyapunov exponents in chaotic systems: their importance and their evaluation using observed data," *Int. J. Mod. Phys. B* **5**, 1347–1375 (1991).
32. D. Nychka, S. Ellner, A. R. Gallant, and D. McCaffrey, "Finding chaos in noisy systems," *J. R. Stat. Soc. B* **54**, 399–426 (1992).
33. D. T. Kaplan and R. J. Cohen, "Is fibrillation chaos?" *Circulation Res.* **67**, 886–892 (1990).
34. R. S. Tsay, "Model checking via parametric bootstraps in time series analysis," *Appl. Stat.* **41**, 1–15 (1992).
35. L. A. Smith, "Identification and prediction of low dimensional dynamics," *Physica D* **58**, 50–76 (1992).
36. J. Theiler, S. Eubank, A. Longtin, B. Galdrikian, and J. D. Farmer, "Testing for nonlinearity in time series: the method of surrogate data," *Physica D* **58**, 77–94 (1992).
37. J. Theiler, P. S. Linsay, and D. M. Rubin, "Detecting nonlinearity in data with long coherence times," in *Time Series Prediction: Forecasting the Future and Understanding the Past. Proceedings of the Workshop held May, 1992, in Santa Fe, New Mexico*, A. S. Weigend and N. A. Gershenfeld, eds. Vol. XVII of *SFI Studies in the Sciences of Complexity*, (Addison-Wesley, 1993), pp. 429–455.
38. B. Efron and R. Tibshirani, "Bootstrap methods for standard errors, confidence intervals, and other measures of statistical accuracy," *Stat. Sci.* **1**, 54–77 (1986).
39. P. Grassberger and I. Procaccia, "Characterization of strange attractors," *Phys. Rev. Lett.* **50**, 346–349 (1983).
40. We chose this version of McLeod-Li as a representative of the "conventional" approach to detecting nonlinearity because it is simple to understand and implement; there are better approaches (see Tong [4]) but these tend to involve massive regressions. Our purpose here is meant to be more illustrative than comparative.
41. We are grateful to William Brock for suggesting this example.
42. M. Berge, "Quantification of chaos in a time series of water levels." Unpublished (1990).
43. B. Townshend, "Nonlinear prediction of speech signals," in *Non-linear Modeling and Forecasting. Proceedings of the Workshop held September, 1990, in Santa Fe, New Mexico*, M. Casdagli and S. Eubank, eds. Vol. XII of *SFI Studies in the Sciences of Complexity*, (Addison-Wesley, 1992), pp. 435–456.

44. E. N. Lorenz, "Deterministic nonperiodic flow," *J. Atmos. Sci.* **20**, 130–141 (1963).
45. O. E. Rössler, "An equation for continuous chaos," *Phys. Lett. A* **57**, 397–398 (1976).
46. J. L. Kaplan and J. A. Yorke, "Chaotic behavior of multidimensional difference equations," in *Functional Differential Equations and Approximations of Fixed Points*, H.-O. Peitgen and H.-O. Walther, eds. Vol. 730 of *Springer Lecture Notes in Mathematics*, (Springer-Verlag, Berlin, 1979), p. 204.
47. The effects of acausal filters are discussed by Mitschke [24] and by Pecora and Carroll [21].
48. T. W. Anderson, *The Statistical Analysis of Time Series*. (Wiley, New York, 1971).
49. A. Čenys, "Lyapunov spectrum of the maps generating identical attractors," *Europhys. Lett.* **21**, 407–411 (1993).
50. M. Casdagli, S. Eubank, J. D. Farmer, and J. Gibson, "State space reconstruction in the presence of noise," *Physica D* **51**, 52–98 (1991).
51. A. M. Fraser and H. L. Swinney, "Independent coordinates for strange attractors from mutual information," *Phys. Rev. A* **33**, 1134–1140 (1986).
52. W. Liebert and H. G. Schuster, "Proper choice of the time delay for the analysis of chaotic time series," *Phys. Lett. A* **142**, 107–111 (1988).
53. Z. Aleksić, "Estimating the embedding dimension," *Physica D* **52**, 362–368 (1991).
54. M. Casdagli, "Chaos and deterministic versus stochastic nonlinear modeling," *J. R. Stat. Soc. B* **54**, 303–328 (1992).
55. D. T. Kaplan and L. Glass, "Direct test for determinism," *Phys. Rev. Lett.* **68**, 427–430 (1992).
56. W. A. Brock. Personal communication.
57. W. A. Brock, J. Lakonishok, and B. LeBaron, "Simple technical trading rules and the stochastic properties of stock returns," *J. Finance* **47**, 1731–1764 (1992).
58. J. D. Scargle, "An introduction to chaotic and random time series analysis," *Int. J. Imaging Syst. Tech.* **1**, 243–253 (1989).
59. J. D. Scargle, "Studies in astronomical time series analysis: IV. Modeling chaotic and random processes with linear filters," *Astrophys. J.* **359**, 469–482 (1990).
60. G. Sugihara and R. May, "Nonlinear forecasting as a way of distinguishing chaos from measurement error in forecasting," *Nature* **344**, 734–741 (1990).